The International Journal of Advanced Manufacturing Technology (2018) 98:2717–2724
https://doi.org/10.1007/s00170-018-2398-7

ORIGINAL ARTICLE

Fatigue analysis of the fiber reinforced additively manufactured objects

A. Imeri[1] · I. Fidan[2] · M. Allen[3] · D. A Wilson[1] · S. Canfield[1]

Received: 8 May 2018 / Accepted: 3 July 2018 / Published online: 23 July 2018

Abstract
This research project analyzes the fatigue properties of fiber-reinforced additively manufactured (FRAM) specimens depending on the effect of fiber orientation, infill type, and composition of FRAM material. Testing specimens with several fiber orientation, infill type, and material compositions were printed using a 3D printer capable of printing with carbon fiber, fiberglass, and Kevlar. Specimens were tested in a tension-tension mode with a stress ratio, $R = 0.1$. The data collected was analyzed with analysis of variance (ANOVA) to investigate the significance of the load, number of rings, and materials on the number of cycles to failure. A number of specimens were tested until they were broken. Highest resistance to failure were of the specimens made of "isotropic" infill carbon fiber with zero and one ring. From the ANOVA results, material, load, and the number of rings are all significant with regard to the number of cycles to failure. ANOVA also showed that load and material interaction were slightly significant to fatigue life. Fiber can be varied for each layer of the specimens, thus changing the mechanical properties of a part. Experiments like these can better the understanding of material properties to improve life of parts under cyclic loading.

Keywords Additive manufacturing · Fiber reinforced additive manufacturing · Composite materials · Mechanical properties · Fatigue · ANOVA

1 Introduction

Among many production technologies, Additive Manufacturing (AM) is one of the latest manufacturing processes. Contrary to the conventional manufacturing that creates waste and leftovers, AM produces near-net shape parts and allows usage of over 90% of the material [1]. The reduction of cost constraint to produce a part is not as significant because the need for complex jigs, fixtures, or moldings is eliminated. Complexity and customization of the parts are also no longer a constraint. AM is being utilized at an increasing rate in sectors such as aerospace and motorsports due to offering high geometrical complexity and short manufacturing lead times [2]. Another main driver of the adoption of AM is the lightweight production of parts [3]. Traditionally, AM has focused on metals and polymers. However, recent techniques like FRAM have widened the scope of material used in AM. Yet, the field of FRAM has been narrowly studied. Generally, the fibers used in FRAM have been discontinuous [4]. In recent years, the Markforged Mark Two (MKF) printer [5] seen in Fig. 1 has appeared on the market and is able to print with continuous fibers. This printer functions by first constructing a matrix of Nylon or Onyx and then overlaying that matrix with fiber filament layer by layer. The pattern in which the fibers are laid down is important, because it changes the structure of the component. Microstructure and macrostructure are crucial for mechanical properties and performance of the parts. Hence, testing the materials for mechanical properties is critical for the utilization of the parts in industry. A very important property is fatigue. Fatigue is officially defined and stated

✉ I. Fidan
ifidan@tntech.edu

A. Imeri
aimeri42@students.tntech.edu

M. Allen
mallen@tntech.edu

D. A Wilson
dwilson@tntech.edu

S. Canfield
scanfield@tntech.edu

[1] Department of Mechanical Engineering, Tennessee Technological University, Cookeville, TN 38505, USA

[2] Department of Manufacturing & Engineering Technology, Tennessee Technological University, Cookeville, TN 38505, USA

[3] Department of Mathematics, Tennessee Technological University, Cookeville, TN 38505, USA

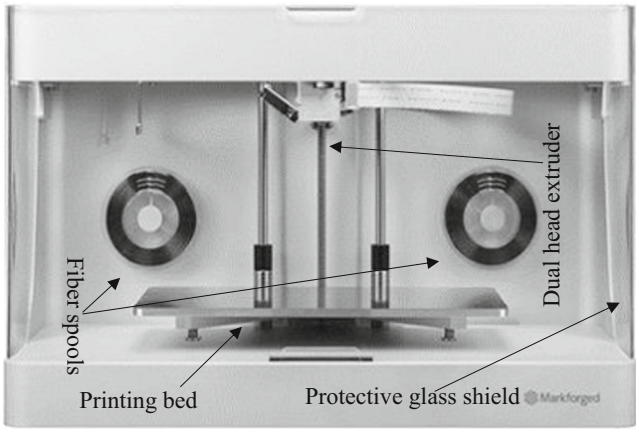

Fig. 1 Markforged Mark Two 3D printer

by the American Society for Testing and Materials [6] as the process of progressive localized permanent structural change occurring in a material subjected to conditions that produce fluctuating stresses and strains at some point or points that may culminate in cracks or complete fracture after a sufficient number of fluctuations. Almost 50–90% of all mechanical failures are fatigue failures [7]. Hence, a thorough investigation in fatigue properties of FRAM materials is paramount for designing parts and systems. However, since continuous FRAM is a new technology, not many of the properties have been tested and analyzed. Dickson et al. [8] evaluated the mechanical performance of FRAM in both tension and flexure. It was demonstrated that carbon fiber-filled specimens did better than fiberglass and Kevlar specimens. Moving to fatigue properties of FRAM materials, Kuchipudi [9] analyzed the effect of the angle of the fiber to the life of the specimens. Specimens with fiber filament layers at 0°, 45°, and 90° were tested under different fiber volumetric fractions. From the results, the specimens with fibers at 0° gave the best results. It should be mentioned that the fiber reinforcement material was fiberglass. Generally, studies have been conducted in conventional polymer materials without fiber reinforcement. Fischer et al. [10] studied the fatigue behavior of FDM Ultem 9085, which is an engineering polymer, printed on Stratasys Type Fortus 400 mc with the independent variable being direction of the print on the print bed. A similar study was conducted with PLA material using Makerbot 2×, where the specimens printed at different bed angles (0°, 45°, and 90°) were tested for fatigue life, with 45° specimens performing slightly better than 0° [11]. Since there is very little data, this study aimed to add to the knowledge base on the effect of different infill patterns and fiber orientations on the fatigue properties of FRAM.

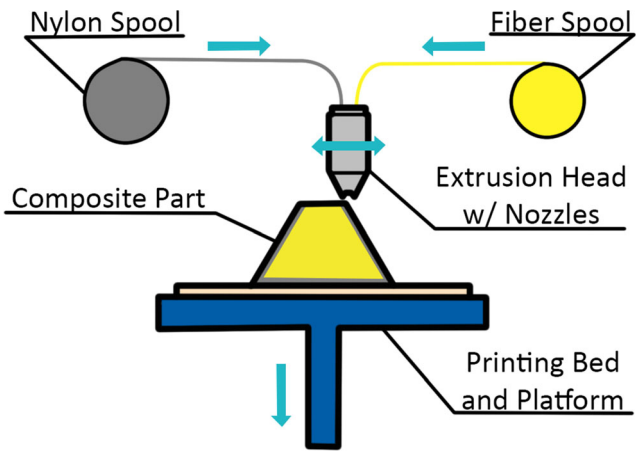

Fig. 2 Schematic of MKF printer extrusion process

2 Methodology

2.1 3D printer

The printer used in this experiment, an MKF printer, has dual head extrusion nozzles which print the base and reinforcement materials, sequentially. To produce a FRAM part, the digital file is needed. This is a 3D solid model part produced with a computer-aided design (CAD) software tool. Then, this file is converted to a .STL file. This STL file is then uploaded to the slicer. The MKF slicer is Eiger, which is a web-based slicer. From the STL file in the slicer, the numerical control code is generated, which commands the printer head what moves to make and when to extrude materials, so the part is produced. A schematic of the printer is shown in Fig. 2. Due to the sensitivity of the materials to moisture, the nylon spool is kept in a watertight Pelican 1430 dry box for protection. The filaments are pulled into the extrusion heads with the help of the stepper motors. The temperature of the extrusion head is between 265 and 270 °C. At this temperature, nylon becomes molten and begins to solidify once it leaves the nozzle. The first layers of the part are nylon. The fiber reinforcement materials, which are not in a molten state, are laid down horizontally layer by layer

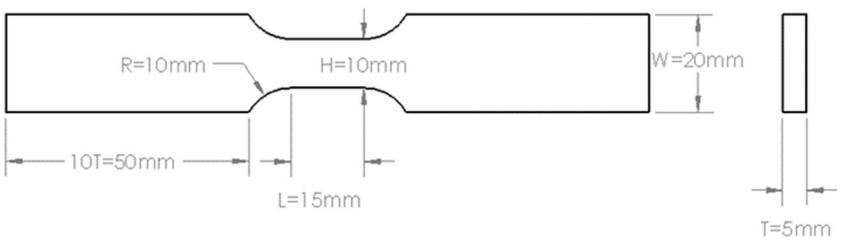

Fig. 3 Fatigue specimen dimensions (ASTM E606M, 2012) [12]

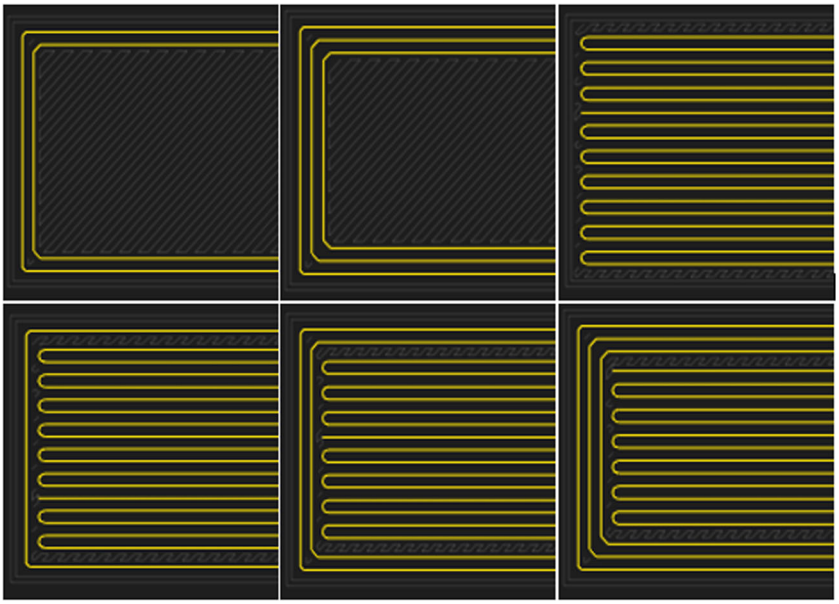

Fig. 4 Top row, from left to right: 2 rings concentric, 3 rings concentric, 0 ring isotropic. Bottom row, from left to right: 1 ring isotropic, 2 rings isotropic, and 3 rings isotropic

into the nylon matrix. The walls or outer borders of the part are also made up of nylon. Therefore, in every layer, the walls are printed first followed by the reinforcement layers, if necessary. This process is concluded with nylon being printed as the final layer. Each part produced using FRAM AM follows this procedure layer by layer.

2.2 Specimen/test model

The ASTM standard used for fatigue testing was E606M [12]. The dimensions of the specimen with are shown in Fig. 3. The ASTM specimens were modeled in SolidWork 2016. All specimens, carbon fiber, Kevlar, and fiberglass were printed with MKF.

For nylon, the infill used in this study was rectilinear, because it shows maximum strength in uniaxial loadings according to [13]. The infill density used is 75%. In the slicing software, a series of controllable settings can be changed, that would also change the specimens' mechanical properties. Fill pattern (triangular, rectilinear, and hexagonal), fill density, total fiber layers, fiber fill type, and concentric fiber rings are just some of the controllable settings. Based on these parameters, there are different specimens with different numbers of rings and different infill types. Based on the type of the fiber reinforcement fill type, specimens can be grouped into two categories. The two categories are concentric and isotropic (not the mechanical properties, but a description of the way fiber is laid down). In the isotropic infill type, rings can also be added conferentially. Just until recently, MKF was the only commercial printer that could print continuous fiber-reinforced parts. Because of this, adding conferential fiber rings and testing for fatigue analysis were firstly conducted in this study.

The cross-section view of the generated different fill types are shown respectively in Fig. 4. The yellow lines represent the fiber reinforcement material, while the black portion represents the nylon. The abbreviation, number of rings and infill type, and description are presented in Table 1.

Table 1 Abbreviations and description of specimens

Abbreviation	No. of rings and fiber fill type	Description
CF/FG/KV-2RC	2 rings concentric	Two concentric rings of fiber in each fiber layer on the nylon matrix
CF/FG/KV-3RC	3 rings concentric	Three concentric rings of fiber in each fiber layer on the nylon matrix
CF/FG/KV-0RI	0 ring isotropic	Isotropic fill with 0° angle direction in each fiber layer on the nylon matrix
CF/FG/KV-1RI	1 ring isotropic	Isotropic fill surrounded by one concentric ring on the outer border of the fiber fill
CF/FG/KV-2RI	2 rings isotropic	Isotropic fill surrounded by two concentric rings on the outer border of the fiber fill
CF/FG/KV-3RI	3 rings isotropic	Isotropic fill surrounded by three concentric rings on the outer border of the fiber fill

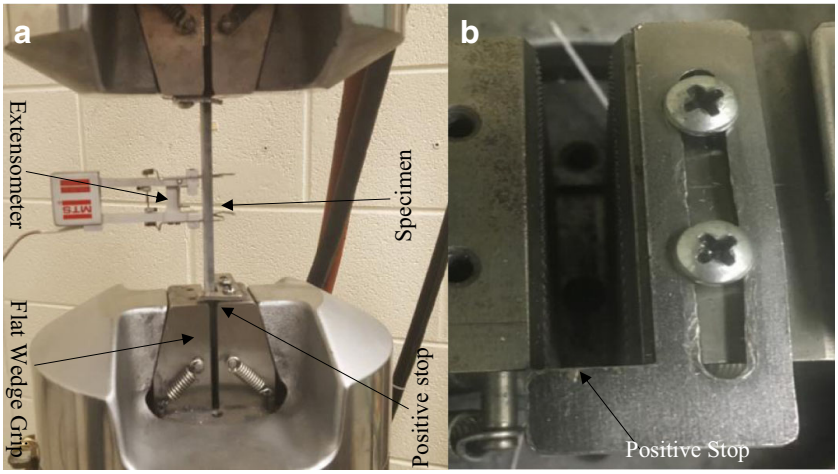

Fig. 5 **a** MTS810 machine. **b** Positive stop

For isotropic specimens, the chosen angle with respect to the horizontal axis is 0°. According to [14], the angle 0° gives better tensile properties. Since the fatigue testing was in a tensile-tensile mode for all isotropic specimens, the fiber angle was set to 0°. Future studies could be conducted with different angles.

2.3 Testing machine

The specimens were tested using a MTS 810 testing machine as seen in Fig. 5a. This model is a closed loop servohydraulic machine. The testing variables, such as frequency, amplitude, and average load, were all controlled and input through MTS's Multipurpose Testware interface. This machine has two gripping heads. The lower head is actuated in order to load the specimen while the upper head is used only for gripping purposes. The gripping pressure applied to the larger portions of the test specimens, Fig. 5b, was 4 MPa. This value was determined since higher gripping pressure caused an immediate crack in the specimens while lower gripping pressure caused the specimen to slip.

3 Results and discussion

3.1 Experimental results

The fatigue experiment for a specimen is concluded when it breaks and is totally separated. The dependent variable is the number of cycles until total separation for the generated specimens. In addition, since the goal of this study is to determine if a correlation exists between geometric orientations and fiber reinforcement material in relation to fatigue properties, some of the specimens that did not break were truncated after 10,000 cycles.

Three specimens of each type presented in Table 1 were produced in order to have a better statistical representation. The type of load for the testing specimens was tensile-tensile load, with a load ratio of 0.1. The Intermediate Value Property Theorem (IVP) [15] was used to determine the magnitude of the loads used for testing. First, high load of 17.4 kN and low load of 3.33 kN were chosen. The logic behind this selection was to eliminate the specimens that would fail immediately. Further, if one specimen failed during the first cycle, meaning that the load is excessive, the second and the third tests were eliminated. Then, intermediate values were also selected and testing was repeated. The testing magnitudes for the maximum loads were 17.4, 13.8, 10.3, and 3.33 kN. Tables 2, 3, 4, and 5 provide a comprehensive summary of all the specimen and load results. These specimens are arranged from the lowest to the highest load. The results of testing at the first load (3.33–0.333 kN) are presented in Table 2.

At this load, the specimens with concentric infill were tabulated only. Isotropic infill specimens did not break at all at this load. From the results, the three-ring concentric infill for any of the materials gave a higher number of cycles. Then, the

Table 2 Results from the first load (3.33–0.33 kN)

Load (kN)	Material	Rings	Type	Test no. 1	Test no. 2	Test no. 3
3.33–0.33	Carbon fiber	2	Concentric	510	222	417
3.33–0.33	Carbon fiber	3	Concentric	10,000+	–	–
3.33–0.33	Kevlar	2	Concentric	45	190	9
3.33–0.33	Kevlar	3	Concentric	383	72	181
3.33–0.33	Fiberglass	2	Concentric	168	132	137
3.33–0.33	Fiberglass	3	Concentric	644	561	644

Table 3 Results from the second load (10.3–1.03 kN)

Load (kN)	Material	Rings	Type	Test no. 1	Test no. 2	Test no. 3
10.3–1.03	Fiberglass	0	Isotropic	750	1161	989
10.3–1.03	Fiberglass	1	Iso + Conc	699	996	744
10.3–1.03	Fiberglass	2	Iso + Conc	19	26	31
10.3–1.03	Fiberglass	3	Iso + Conc	1	–	–
10.3–1.03	Carbon fiber	0	Isotropic	10,000+	–	–
10.3–1.03	Carbon fiber	1	Iso + Conc	10,000+	–	–
10.3–1.03	Carbon fiber	2	Iso + Conc	3753	3995	1747
10.3–1.03	Carbon fiber	3	Iso + Conc	1	1	
10.3–1.03	Kevlar	0	Isotropic	10,000+	–	–
10.3–1.03	Kevlar	1	Iso + Conc	54	285	196
10.3–1.03	Kevlar	2	Iso + Conc	1	–	–
10.3–1.03	Kevlar	3	Iso + Conc	1	–	–
10.3–1.03	Carbon fiber	3	Concentric	1	–	–
10.3–1.03	Fiberglass	3	Concentric	1	–	–

three-ring isotropic specimens were then tested at the second load. The second load (10.3–1.03 kN) results are shown in Table 3; the concentric specimens with three rings, that showed a higher number of cycles in the first load, failed in the first cycle.

Except the three-ring concentric specimens failing in the first cycles, in the second load too, the isotropic specimen with three concentric rings for any material failed in the first cycle. The Kevlar specimens with two-ring isotropic infill, contrary to fiberglass and carbon fiber specimens, failed in the first cycle. Kevlar and fiberglass isotropic with concentric one ring failed within a range of cycles under 10,000 (the truncating number of cycles). However, carbon fiber specimen did not break in that range.

After truncating the specimens from the previous load, in the 13.8–1.38 kN, the isotropic with concentric two-ring specimens of carbon fiber and fiberglass failed in the first cycle. Kevlar specimens with one-ring isotropic infill failed in the first cycle, while isotropic with zero rings had just a small number of cycles. The only specimens that had more than 10,000 cycles were the carbon fiber with zero rings. Results are presented in Table 4.

For the highest load case, the 17.4–1.74 kN, testing all other specimens failed in the first cycle other than carbon fiber specimens with no rings. However, even in these specimens, a cracking sound was heard in the first cycle. Results from the final load are presented in Table 5.

3.2 Results of the data analysis

The analysis of the data was achieved by applying a full-factorial ANOVA design. The dependent variable was the number of cycles until failure, while the independent variables were load, material, rings, and type of infill. Since the data were counts, i.e., discrete, a log transformation of the dependent variable was performed. Also, extreme counts led to a right truncation because the MTS 810 stopped after 10,000 cycles. Moreover, depending on the load, some specimens failed in the first cycle, i.e., left truncated. Therefore, the full-factorial ANOVA was reduced to a four-way ANOVA with missing data. Because of the robustness of the ANOVA procedure, the removal of these truncated data had little effect on the overall power of the test. In all the cases, the ANOVA results were well within the boundaries for a classical

Table 4 Results from the third load (13.8–1.38 kN)

Load (kN)	Material	Rings	Type	Test no. 1	Test no. 2	Test no. 3
13.8–1.38	Fiberglass	0	Isotropic	5	66	20
13.8–1.38	Fiberglass	1	Iso + Conc	15	24	38
13.8–1.38	Fiberglass	2	Iso + Conc	1	–	–
13.8–1.38	Carbon fiber	0	Isotropic	10,000+	–	–
13.8–1.38	Carbon fiber	1	Iso + Conc	324	275	209
13.8–1.38	Carbon fiber	2	Iso + Conc	1	–	–
13.8–1.38	Kevlar	0	Isotropic	3	7	6
13.8–1.38	Kevlar	1	Iso + Conc	1	–	–

Table 5 Results from the fourth load (17.4–1.74 kN)

Load (kN)	Material	Rings	Type	Test no. 1	Test no. 2	Test no. 3
17.4–1.74	Fiberglass	0	Isotropic	1	–	–
17.4–1.74	Fiberglass	1	Iso + Conc	1	–	–
17.4–1.74	Carbon fiber	0	Isotropic	19	4	12
17.4–1.74	Carbon fiber	1	Iso + Conc	1	–	–
17.4–1.74	Carbon fiber	2	Iso + Conc	1	–	–
17.4–1.74	Kevlar	0	Isotropic	1	–	–

ANOVA, meaning the assumptions of normality and homogeneous variance were not violated. Although the results of the original ANOVA experiment with no truncation could have been used, the best model was the one with both left and right truncations and that model is presented here. There was one violation to the classical model which was resolved. The independent variable rings and types of infill were found to be overlapping, meaning the two variables were correlated. The variable rings were found to be more influential. Hence, type of infill was not included in the analysis. Results from the ANOVA studies are presented in Table 6. It can be seen that load, material, and rings all have a significant value in the number of cycles while the interaction of load and material is slightly significant.

To make this more understandable, a group of graphs depicting the boxplots for the number of cycles for each treatment level in each dependent variable is provided. The box plot graph of number of log cycles versus three types of loads, starting from load 2 (10.3–1.03 kN), load 3 (13.8–1.38 kN), and load 4 (17.4–1.74 kN) is shown in Fig. 6.

From this figure, it can be seen that regardless of material at different loads, from all data, a "S-N"-like curve is generated. The thick line represents the median; in each case, the median is higher than the number of maximum cycles in the other load, from right to left. This explains the importance of the load in the variance of the number of cycles. Next, the number of cycles versus the number of rings is presented in Fig. 7.

For the three and one numbers of rings specimens, it can be understood that the median of the cycles has more cycles than the most of two and zero numbers of rings. However, while testing at higher loads, it was seen that the isotropic with concentric three rings would fail early, but at the first load (3.33–0.33 kN) in concentric infill type, three rings were giving a higher number of cycles. So, that high number of cycles is for concentric infill types.

Finally, for completeness, more fiberglass specimens with an isotropic infill and zero rings were tested at the following loads, 3338–334 N, 2888–289 N, and 2550–255 N. Even though more data is necessary for a full model, a preliminary S-N curve could be fitted here. The fiberglass zero isotropic S-N curve is shown in Fig. 8. Non-linear regression was applied to the given data with a formula:

$$\text{load} = 3547 \times \exp(0.0004 \times \text{cycles}) \quad (1)$$

Table 6 Results from analysis of variance

	Df	Sum Sq	Mean Sq	*F* value	*p* value
Load	3	46.542	15.5141	31.894	3.58E-09
Material	2	33.521	16.7607	34.4567	2.82E-08
Rings	3	27.645	9.2149	18.944	6.57E-07
Load × material	2	4.331	2.1653	4.4514	0.02096
Residuals	28	13.62	0.4864		

3.3 Discussion

Specimens of nylon reinforced with carbon fiber, fiberglass, or Kevlar were printed with different infill types. These specimens were tested at four different loads with a load ratio (*R*) of 0.1.

In the first type of infill, three-ring specimens performed better than the two-ring specimens. This could be due the different fiber volumetric fractions: more fiber means stronger parts. For the same reason, concentric infill specimens failed in the other loads.

Hence, it can be concluded that for low loads, such as the 3.33–0.33 kN, concentric type infill works well. Additionally, to make a part more resistant to failure due to fatigue, the

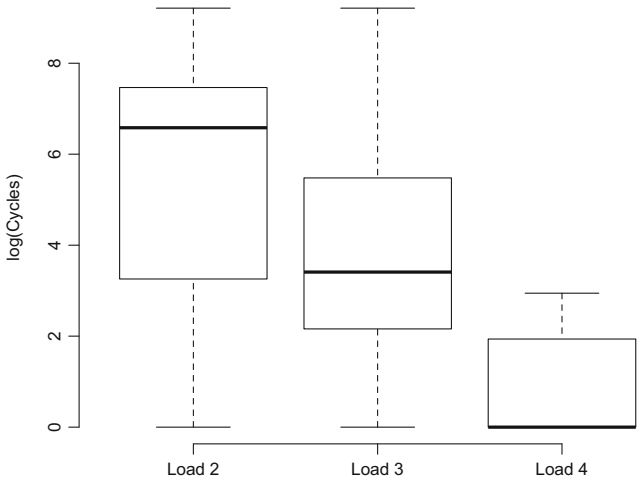

Fig. 6 Number of cycles versus varying fiber reinforcement material

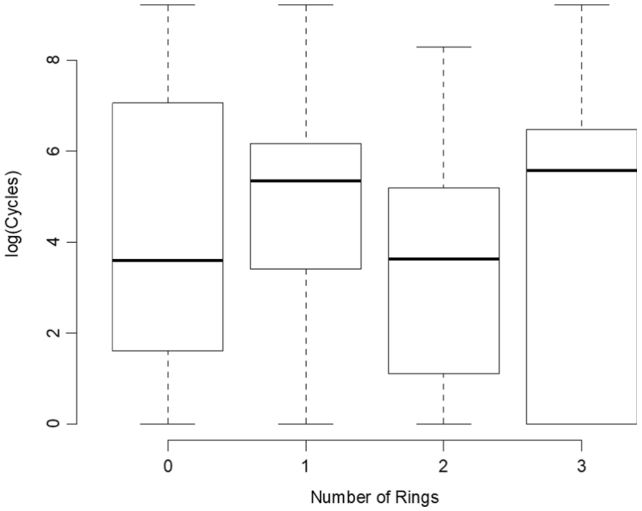

Fig. 7 Number of cycles versus number of rings

number of rings can be increased up to the geometric limit for concentric infill. The ANOVA results supported this claim, where in Fig. 6, the number of cycles with three concentric rings stands higher than the others.

In the isotropic infill type with rings or no ring, generally the fiber volumetric fraction is the same (difference less than 0.1 cm^3), thus, meaning that the fiber orientation and number of rings have a significant effect. This is showed by the experimental and statistical results. At all the remaining three loads, with isotropic infill, increasing the number of rings proved to decrease the number of cycles to failure. Also, the type of material is very important as the fibers seem to carry the majority of the load. From ANOVA too, it results that the material has a significant importance in the number of cycles. Generally, as seen from Tables 3, 4, and 5, carbon fiber

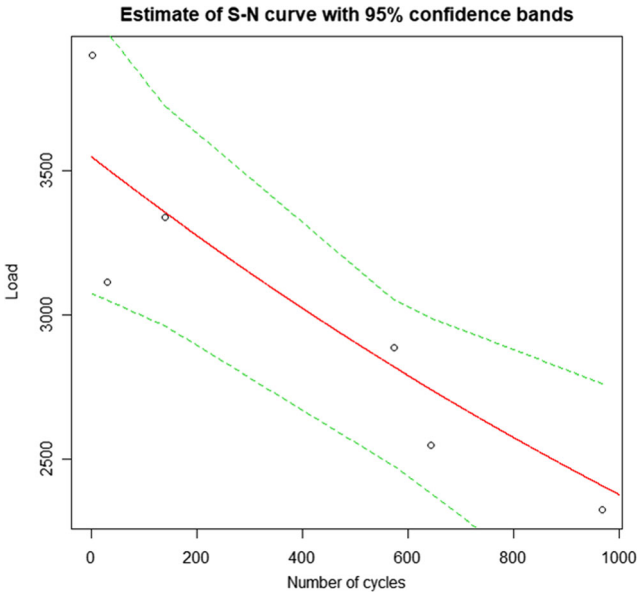

Fig. 8 S-N curve for fiberglass with 0 rings isotropic fill

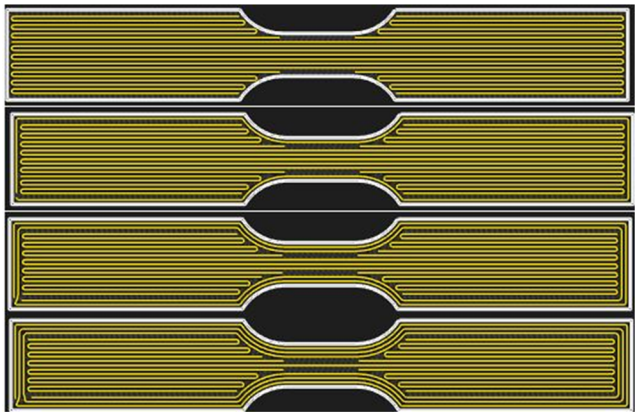

Fig. 9 From top to bottom, isotropic specimens with 0, 1, 2, and 3 rings, respectively

specimens perform better than fiberglass and Kevlar specimens, with Kevlar being the weakest.

The fiber orientation becomes very important in the narrow area of the specimen. Since the cross-sectional area is smaller, the stress is larger in that region. Thus, it is important to analyze the fiber orientation in the cross-sectional area. The horizontal cross-sectional view of the isotropic specimens with a different number of rings is shown in Fig. 9.

It can be seen in the narrower region: when more rings are added, the horizontal isotropic fiber area decreases. The more the isotropic fiber area decreases, the lower the failure resistance.

Generally, the failure mode for all the specimens was fiber pullout. The amount of fiber pullout differed with various loads. Before breaking, fiberglass and Kevlar with nylon specimens would deflect more than carbon fiber with nylon. Failed specimens of different materials at 10.34–1.03 kN are shown in Fig. 10.

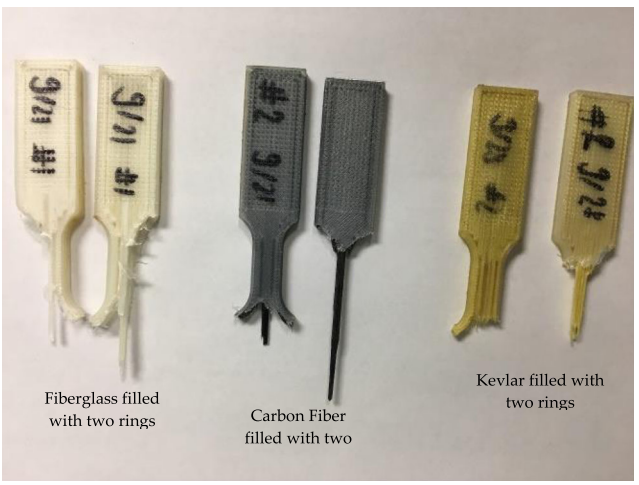

Fig. 10 Fiberglass, carbon fiber, and Kevlar broken specimens at the same load

4 Conclusion

The experiments showed that there is a correlation between filler material type and the pattern the reinforcing material is extruded. Among the materials tested carbon fiber was shown to have better fatigue resistance than the other reinforcing materials. For concentric infill, adding more rings improves the fatigue life of the specimen. While for isotropic infill, increasing the number of rings weakens the fatigue performance. In addition, this study revealed that the isotropic with zero rings and one ring isotropic with concentric infill types showed better results. Furthermore, the experimental results are supported by ANOVA. Number of cycles is strongly dependent from the load, number of rings, and materials. Also, all data, fit an S-N curve. The load and material interaction effect are also significant. Hence, varying any of these parameters significantly changes the properties of a part. Finally, the novelty about this study is that it showed that parts can perform better if conferential rings are added, besides the conventional method of changing the angle of fibers only.

Funding information This work is part of a larger project funded by the Advanced Technological Education Program of the National Science Foundation, DUE no. 1601587. The funding provided by the National Science Foundation is greatly appreciated.

References

1. Swolfs Y, Pinho ST (2016) Designing and 3D printing continuous fibre-reinforced composites with a high fracture toughness. In Proceedings of the 31st Technical Conference of the American Society for Composites. DESTech Publications, pp 1–8
2. Rawal S, Brantley J, Karabudak N (2013) Additive manufacturing of Ti–6Al–4V alloy components for spacecraft applications. In Recent Advances in Space Technologies (RAST), 2013 6th International Conference. IEEE, pp 5–11
3. Huang R, Riddle M, Graziano D, Warren J, Das S, Nimbalkar S, Cresko J, Masanet E (2016) Energy and emissions saving potential of additive manufacturing: the case of lightweight aircraft components. J Clean Prod 135:1559–1570
4. Quan Z, Wu A, Keefe M, Qin X, Yu J, Suhr J, Byun JH, Kim BS, Chou TW (2015) Additive manufacturing of multi-directional preforms for composites: opportunities and challenges. Mater Today 18(9):503–512
5. Markforged [Online] https://markforged.com/about/ [Accessed on November 2, 2017]
6. ASTM E1823-13 (2013) Standard terminology relating to fatigue and fracture testing. ASTM International, West Conshohocken, p 1034 www.astm.org
7. Stephens et al (2001) Metal fatigue in engineering, 2nd edn. Wiley, New York
8. Dickson et al (2017) Fabrication of continuous carbon, glass and Kevlar fibre reinforced polymer composites using additive manufacturing. Addit Manuf 16:146–152
9. Kuchipudi SCH (2017) The effects of fiber orientation and volume fraction of fiber on mechanical properties of additively manufactured composite material, M.S Thesis, Minnesota State University, viewed on 31 January, 2018, <https://cornerstone.lib.mnsu.edu/cgi/viewcontent.cgi?article=1732&context=etds>
10. Fischer M, Schöppner V (2017) Fatigue behavior of FDM parts manufactured with Ultem 9085. JOM 69:563–568. https://doi.org/10.1007/s11837-016-2197-2
11. Letcher T, Waytashek M (2014) Material property testing of 3D-printed specimen in PLA on an entry-level 3D printer. In ASME 2014 international mechanical engineering congress and exposition. American Society of Mechanical Engineers, pp V02AT02A014–V02AT02A014
12. ASTM E606/E606M-12 (2012) Standard test method for strain-controlled fatigue testing. ASTM International, West Conshohocken www.astm.org
13. Fernandez-Vicente M, Calle W, Ferrandiz S, Conejero A (2016) Effect of infill parameters on tensile mechanical behavior in desktop 3D printing. 3D Printing and Additive Manufacturing 3(3):183–192
14. Campbell FC (2010) Structural composite materials. A S M International, Materials Park, p 444
15. Stewart J (2011) Multivariable calculus, international metric edition, (7th ed., International ed., Metric version. ed.):p.23. Brooks Cole - M.U.A